Effects of the entrance channel and fission barrier in the synthesis of superheavy element $Z = 120$

A. K. Nasirov,[1,2] G. Mandaglio,[3,4] G. Giardina,[3,4] A. Sobiczewski,[5] and A. I. Muminov[2]
[1]*Joint Institute for Nuclear Research, Joliot-Curie 6, Dubna 141980, Russia*
[2]*Institute of Nuclear Physics, Ulugbek, 100214 Tashkent, Uzbekistan*
[3]*Dipartimento di Fisica dell' Università di Messina, Salita Sperone 31, 98166 Messina, Italy*
[4]*Istituto Nazionale di Fisica Nucleare, Sezione di Catania, Via S. Sofia, 64, 95123 Catania, Italy*
[5]*Soltan Institute for Nuclear Studies, Hoza 69, PL-00-681 Warsaw, Poland*
(Received 8 September 2011; published 19 October 2011)

The fusion and evaporation residue cross sections for the ^{50}Ti+^{249}Cf and ^{54}Cr+^{248}Cm reactions calculated by the combined dinuclear system and advanced statistical models are compared. These reactions are considered to be used to synthesize the heaviest superheavy element. The ^{50}Ti+^{249}Cf reaction is more mass asymmetric than ^{54}Cr+^{248}Cm, and the fusion excitation function for the former reaction is higher than the one for the latter reaction. The evaporation residue excitation functions for the mass asymmetric reaction is higher in comparison with the one for the ^{54}Cr+^{248}Cm reaction. The use of the mass values of superheavy nuclei calculated in the framework of the macroscopic-microscopic model by the Warsaw Group [Muntian, Z. Patyk, and A. Sobiczewski, Phys. At. Nuclei **66**, 1015 (2003)] leads to a smaller evaporation residue cross section for both the reactions in comparison with the case of using the masses calculated by Möller and Nix [J. Phys. G: Nucl. Part. Phys. **20**, 1681 (1994)]. The ^{50}Ti+^{249}Cf reaction is more favorable in comparison with the ^{54}Cr+^{248}Cm reaction: the maximum values of the excitation function of the $3n$ channel of the evaporation residue formation for the ^{50}Ti+^{249}Cf and ^{54}Cr+^{248}Cm reactions are about 0.1 and 0.07 pb, respectively, but the yield of the $4n$ channel for the former reaction is lower (0.004 pb) in comparison with the one (0.01 pb) for the latter reaction.

DOI: 10.1103/PhysRevC.84.044612 PACS number(s): 25.70.Jj, 25.70.Gh, 25.85.−w, 27.90.+b

I. INTRODUCTION

The synthesis of the superheavy elements with $Z = 114$ to 118 by hot-fusion reactions of ^{48}Ca with actinide targets [1,2] and with $Z = 110$, 111, and 112 by using cold-fusion reactions [3,4] with lead- and bismuth-based targets (shell closed spherical nuclei) have been reported. The cross section of the evaporation residue (ER) formation being a superheavy element is very small: some picobarns, or even the part of a picobarn. The lightest isotope ^{278}113 of the superheavy element $Z = 113$ which was synthesized in the cold-fusion ^{70}Zn+^{209}Bi reaction was observed with a cross section value equal to some percent of a picobarn [4].

To find favorable reactions (projectile and target pair) and the optimal beam energy range leading to larger cross sections of synthesis of superheavy elements, we should establish conditions leading to increase as much as possible the events of ER formation. The ER formation process is often considered as the third stage of the reaction mechanism in heavy ion collisions near the Coulomb barrier energies. The first stage is a capture—formation of the dinuclear system (DNS) after full momentum transfer of the relative motion of colliding nuclei into the shape deformation, excitation energy, and rotational energy of nuclei. The capture takes place if the initial energy of the projectile in the center-of-mass system is sufficiently large to overcome the interaction barrier (Coulomb barrier + rotational energy of the entrance channel), and it is dissipated leading to trap the DNS into the well of the nucleus-nucleus interaction potential [5]. The same mechanism takes place in both kinds of reactions, but the probability of the realization of each stage of the whole mechanism is different in cold- and hot-fusion reactions [6].

We calculate the cross section of the ER formed after each step x of the de-excitation cascade after the emission from the hot compound nucleus (CN) of the particles $\nu(x)n + y(x)p + k(x)\alpha + s(x)\gamma$ [where $\nu(x)$, y, k, and s are the numbers of neutrons, protons, α particles, and γ quanta, respectively] by formula (see Refs. [5,7]):

$$\sigma_{\rm ER}(E_{\rm c.m.}) = \Sigma_{\ell=0}^{\ell_d}(2\ell+1)\sigma_{\ell}^{(x-1)}(E_{\rm c.m.}) \times W_{\rm sur}^{(x-1)}(E_{\rm c.m.} + Q_{\rm gg}, \ell), \quad (1)$$

where $\sigma_{\ell}^{(x-1)}$ is the partial formation cross section of the excited intermediate nucleus of the $(x-1)$th step, and $W_{\rm sur}^{(x-1)}$ is the survival probability of the $(x-1)$th intermediate nucleus against fission along the de-excitation cascade of the CN. It is clear that the first de-excitation step occurs with the compound nucleus which is formed at complete fusion:

$$\sigma_{\ell}^{(0)}(E_{\rm c.m.}, \ell) = \sigma_{\rm fus}(E_{\rm c.m.}, \ell). \quad (2)$$

The fusion cross section is related to the number of events corresponding to the transformation of the dinuclear system into compound nucleus in competition with the quasifission process. It is defined by the product of the partial capture cross section and the related fusion factor $P_{\rm CN}$ which allows us to take into account the competition between the complete fusion and quasifission processes (see Refs. [8,9]):

$$\sigma_{\rm fus}(E_{\rm c.m.}, \ell) = \sigma_{\rm capture}(E_{\rm c.m.}, \ell)P_{\rm CN}(E_{\rm c.m.}, \ell). \quad (3)$$

Our method of calculation (also including the advanced statistical method [10–12]) of the ER cross sections takes into account the damping of the shell correction in the fission barrier as a function of the excitation energy and orbital angular momentum. This is accounted for by the various steps of the

de-excitation cascade of the compound nucleus leading to the fission fragments or the ER nuclei in the exit channel [7,13,14].

The study of the dynamics of these processes in heavy ion collisions near the Coulomb barrier energies showed that complete fusion does not occur immediately in the case of massive nuclei collisions [7–9,15,16]. The quasifission process competes with the formation of the CN. This process occurs when the DNS prefers to break down into two fragments instead of being transformed into the fully equilibriated CN. The number of events undergoing quasifission increases drastically by increasing the sum of the Coulomb interaction and rotational energy in the entrance channel [5,17]. The Coulomb interaction increases by increasing the charge number of the projectile or target nucleus, as well as by decreasing the charge asymmetry of colliding nuclei at the fixed total charge number of the DNS.

Another reason for decreasing the yield of the ER is the fission of a heated and rotating CN which is formed in competition with quasifission. The stability of a massive CN decreases due to the decrease of the fission barrier by increasing its excitation energy $E^*_{\rm CN}$ and angular momentum ℓ [10–12]. The stability of the transfermium nuclei is connected with the red appearance of the shell correction in their binding energy [18], which is sensitive to the angular momentum and $E^*_{\rm CN}$ values. The fusion-fission takes place when the compound nucleus cannot survive against fission due to the smallness of its fission barrier which decreases by increasing the excitation energy $E^*_{\rm CN}$ and/or angular momentum $\ell_{\rm CN}$. In the cold-fusion reactions the desired flow of nucleons from the projectile nucleus to the target nucleus (in this case ^{208}Pb or ^{209}Bi) is strongly hindered when the projectile is heavier than ^{70}Zn. This is connected with the dependence of the potential energy surface (PES) on the mass and charge asymmetries and on the shell effects in the binding energies of colliding nuclei (see Fig. 1). The use of nuclear binding energies including shell effects in calculations of the PES and the driving potential of the DNS leads to the appearance of hollows on the PES around the charge and mass symmetries corresponding to the constituents of the DNS with the magic proton or/and neutron numbers (see Figs. 4 and 5 in Ref. [5]).

The charge asymmetry of the entrance channel for the "cold-fusion" reactions is placed on the hollow between the Businaro-Gallone point b in Fig. 1 and the valley of the charge symmetric channel (point d in Fig. 1). The intrinsic fusion barrier $B^*_{\rm fus}$ increases by increasing the projectile charge and mass numbers. It is determined as the difference between the values of the potential energy surface on the point where the DNS had been captured (on the bottom of the potential well of the nucleus-nucleus interaction considered as a function of the relative distance R between the centers of the nuclei) and on the "saddle point" in the fusion valley (near point b of Fig. 1) (for details see Refs. [5,19,20]). This fact leads to a strong increase of the hindrance to complete fusion, and the probability of compound nucleus formation becomes very small.

The superheavy elements $Z = 110$, 111, 112, and 113 were synthesized in cold-fusion reactions by bombarding ^{208}Pb and ^{209}Bi nuclei which have $N = 126$ neutrons. The cold-fusion reactions were preferable for the synthesis of superheavy

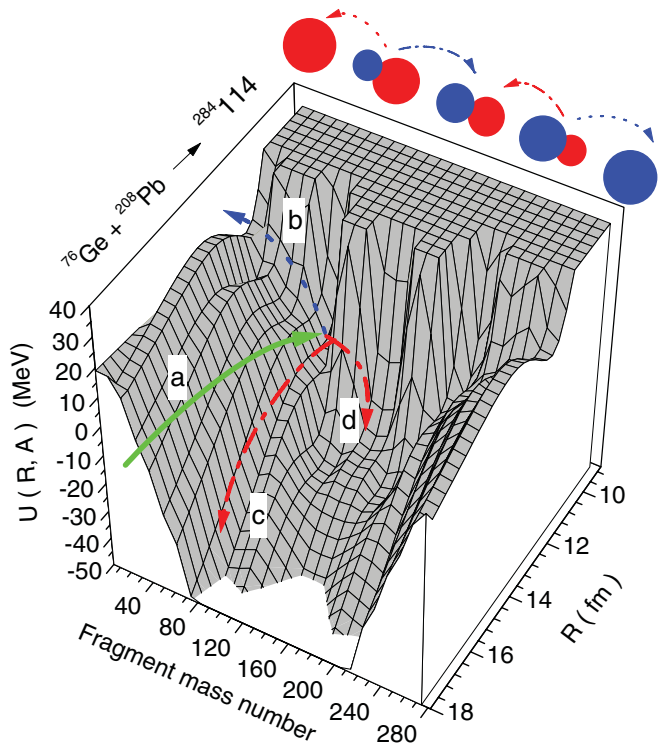

FIG. 1. (Color online) Potential energy surface calculated for the DNS leading to the formation of the ^{284}114 compound nucleus as a function of the relative distance between the centers of mass of the interacting nuclei and the mass number of a fragment.

elements up to $Z = 112$. For example, the maximum value of the ER cross section ($\sigma_{\rm ER}$) at the synthesis of the superheavy element $^{265}_{108}$Hs in the cold-fusion reaction ^{58}Fe+^{208}Pb [21] was $\sigma_{\rm ER} = 65$ pb. This value is about one order of magnitude higher than the ER cross section $\sigma_{\rm ER} = 7$ pb measured in the hot-fusion reaction ^{28}Si+^{238}U [16], but the synthesis of superheavy elements becomes more favorable in hot-fusion reactions starting from $Z = 112$.

Therefore, all of the last group of elements with $Z = 114$, 115, 116, 117, and 118 were synthesized in the hot-fusion reactions where the actinide targets ^{242,244}Pu, ^{243}Am, ^{248}Cm, ^{249}Bk, and ^{249}Cf were bombarded by the neutron rich isotope ^{48}Ca.

II. ADVANTAGE OF HOT-FUSION REACTIONS WITH MASSIVE NUCLEI

The advantage of hot-fusion reactions in comparison with cold-fusion reactions is connected with the relatively small hindrance in the compound nucleus formation. Because the charge asymmetry of the entrance channel (^{48}Ca) in hot-fusion reactions is placed closer to the Businaro-Gallone point (see Fig. 1), consequently the intrinsic fusion barrier $B^*_{\rm fus}$ of the DNS is smaller in comparison with the one for cold-fusion reactions (^{76}Ge). The large excitation energy of the compound nucleus is an inevitable circumstance in the hot-fusion reactions because after capture and formation of the DNS, the value of the PES corresponding to the entrance

TABLE I. Comparison of the fusion probabilities P_{CN} for the cold- (left side) and hot- (right side) fusion reactions calculated in the dinuclear system model [5,19,20]

Cold-fusion reactions	Z_{CN}	$\eta = \frac{A_2-A_1}{A_1+A_2}$	$P_{CN} \times 10^{-8}$	Hot-fusion reactions	Z_{CN}	$\eta = \frac{A_2-A_1}{A_1+A_2}$	$P_{CN} \times 10^{-2}$
^{64}Ni+^{208}Pb[a]	110	0.529	14.0	^{48}Ca+^{243}Am[b]	115	0.670	5.02
^{64}Ni+^{209}Bi[a]	111	0.531	7.0	^{48}Ca+^{248}Cm[b]	116	0.676	1.13
^{70}Zn+^{208}Pb[a]	112	0.496	0.25	^{48}Ca+^{249}Bk[c]	117	0.677	2.06
^{70}Zn+^{209}Bi[a]	113	0.498	0.052	^{50}Ti+^{249}Cf[c]	120	0.666	0.112
^{76}Ge+^{208}Pb[a]	114	0.465	0.012	^{54}Cr+^{248}Cm[c]	120	0.642	0.0231

[a]The estimations made from the results of Ref. [5].
[b]The estimations made from the results of Ref. [7].
[c]The estimations made from this work.

channel charge asymmetry is settled at higher points of its hollow in comparison with the case of cold-fusion reactions. Therefore, even if the compound nucleus is formed by the minimum possible energy beam, it is excited at energies higher than 30 MeV. As an example, to show such a strong difference of the hindrance to complete fusion, we compare in Table I the values of fusion probability (P_{CN}) for two sets of the cold and hot-fusion reactions.

The small cross section of the ER formation in hot-fusion reactions is connected with the small survival probability against fission ($W_{surv} \approx 10^{-8}$) of the heated and rotating compound nucleus. The synthesis of superheavy elements with $Z = 117$ and 118 at the Flerov Laboratory of Nuclear Reactions of JINR in Dubna, Russia, as well as the confirmation of the Dubna Group's results for the new elements with $Z = 114$ and 116 at the Lawrence Berkeley National Laboratory, USA, [22] and at GSI, Darmstadt, Germany, [23] by the SHIP Group, caused the new attempts to reach a heavier element, $Z = 120$. Theoretical estimations of the ER cross sections for the ^{54}Cr+^{248}Cm, ^{58}Fe+^{244}Pu, and ^{64}Ni+^{238}U reactions have already been made in Refs. [19,24–26]. In the experiment with the ^{58}Fe+^{244}Pu reaction, which was reported in Ref. [27], no event for the synthesis of the $Z = 120$ element was observed: the upper limit of the cross section of 0.4 pb at $E^*_{CN} = 46.7$ MeV was estimated. The results of two experiments at GSI, where the ^{64}Ni+^{238}U reaction was used, did not show events for the synthesis of the $Z = 120$ element. The ^{54}Cr+^{248}Cm reaction, which seems to be the most favorable among the above-mentioned reactions, was recently performed at GSI.

In Table II, the predictions of the maximum values of the evaporation residues excitation functions for the $3n$ and $4n$ channels by different models (see Refs. [24–26,28] are presented. The results presented in Refs. [24–26] were obtained by using the theoretical binding energies from the mass table by P. Möller *et al.* [29], while the authors of Ref. [28] have used the mass data calculated by Warsaw Group [30].

The difference between compared results in Table II can be explained by three main reasons: (1) the authors used different methods to estimate the formation probability of the heated and rotating compound nuclei ^{299}120 and ^{302}120 in the ^{50}Ti+^{249}Cf and ^{54}Cr+^{248}Cm reactions (details of the calculations can be found in the corresponding references); (2) the survival probability calculations of the compound nucleus against fission are sensitive to the values of the statistical model parameters; and (3) the use of different theoretical nuclear mass tables can give the relevant difference in the values of nuclear binding energy.

The theoretical results obtained by the Warsaw Group within the macroscopic-microscopic model [31,32] showed the increase of the fission barrier of the isotopes of the superheavy element $Z = 120$ while decreasing its mass number from the value $A = 310$ down to $A = 296$ (see Fig. 2). This

TABLE II. Comparison of the predicted maximum values of the evaporation residues cross section (σ_{ER}) in the ^{54}Cr+^{248}Cm and ^{50}Ti+^{249}Cf reactions obtained in Refs. [24–26,28] with our results for the 3- and 4-neutrons emission channels as a function of the collision energy in the center-of-mass system $E_{c.m.}$. The presented data about maximum values from Refs. [24–26,28] were extracted from the figures of the ER excitation functions.

	^{50}Ti+^{249}Cf			^{54}Cr+^{248}Cm				Reference
$E_{c.m.}$ (MeV)	$\sigma^{(3n)}_{ER}$ (fb)	$E_{c.m.}$ (MeV)	$\sigma^{(4n)}_{ER}$ (fb)	$E_{c.m.}$ (MeV)	$\sigma^{(3n)}_{ER}$ (fb)	$E_{c.m.}$ (MeV)	$\sigma^{(4n)}_{ER}$ (fb)	
236.0	1.5			248.2	0.2			[26][a]
236.0	40.0	241.0	46.0	246.7	14.0	249.6	28.0	[25][a]
231.5	60.0	232.5	40.0					[24][a]
227.5	760.0	239.0	28.0	241.5	76.0	252.0	12.0	[28][b]
225.0	100.0	231.5	2.5	237.2	55.0	241.0	13.0	This work[a]

[a]The corresponding authors used data from the mass table presented in Ref. [29].
[b]The corresponding authors used data from the mass table presented in Ref. [30].

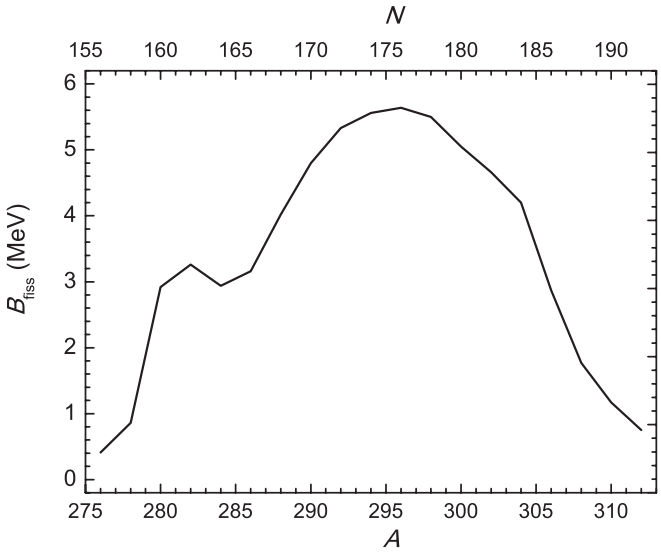

FIG. 2. Fission barriers for the isotopes of superheavy element $Z = 120$ calculated by the macroscopic-microscopic model of Ref. [32].

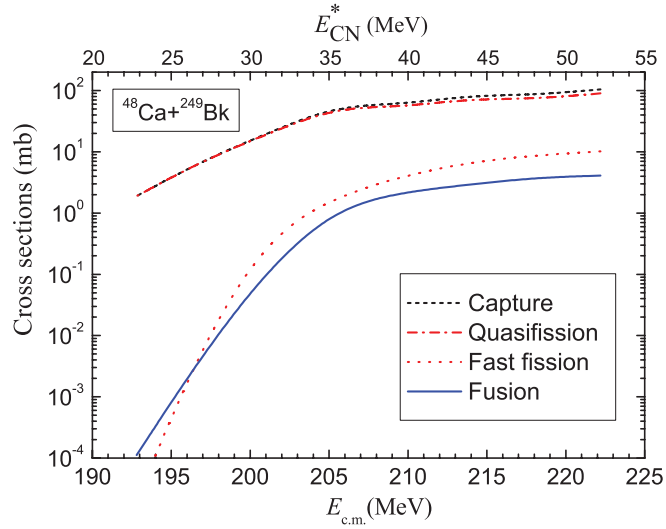

FIG. 3. (Color online) Capture (dashed line), quasifission (dotted-dashed line), fast fission (dotted line), and fusion (solid line) cross sections calculated by the DNS model [17,20,33] for the ^{48}Ca+^{249}Bk reaction. The excitation energy E^*_{CN} of the compound nucleus (top axis) is calculated by the use of the Möller and Nix mass table [29].

effect was obtained by taking into account nonaxial quadrupole deformation. Therefore, we estimated in this paper the ER cross sections for the ^{50}Ti+^{249}Cf reaction leading to formation of the isotope $A = 299$ of the $Z = 120$ element to observe the effect of the increasing barrier on the ER formation. In Section III, we compare our results of capture, fusion, and evaporation residue cross sections for the ^{50}Ti+^{249}Cf and ^{54}Cr+^{248}Cm reactions to find out the role of the entrance channel and fission barriers on the reaction products.

III. CAPTURE, FUSION, AND EVAPORATION RESIDUE CROSS SECTIONS FOR THE ^{50}Ti+^{249}Cf AND ^{54}Cr+^{248}Cm REACTIONS

The calculations of capture and fusion cross sections were performed in the framework of the DNS model. The details of this model can be found in Refs. [7,19,20,33]. The partial fusion cross sections $\sigma^{(\ell)}_{fus}$ obtained in the DNS model were used to calculate evaporation residue cross sections by the advanced statistical model [11,12]. We have described the experimental data [34] of the ER cross section for the ^{48}Ca+^{249}Bk reaction leading to the superheavy element $Z = 117$. The results of calculations for the capture and fusion cross sections for the ^{48}Ca+^{249}Bk reactions are presented in Fig. 3.

The capture of the projectile by the target at a given beam energy and for all possible orbital angular momentum values is determined as the trapping of the system into a potential well of the nucleus-nucleus interaction after full momentum transfer and dissipation of the relative kinetic energy into the deformation and excitation energy of nuclei (for details see Refs. [17,20,33]). The number of partial waves contributing to the capture cross section is found by solution of the classical equation of motion for the relative distance between centers of the interacting nuclei and the angular momentum [20]. The friction coefficients are calculated by using the expression obtained by averaging the coupling term between intrinsic excitation in nuclei and nucleon exchange between them [35].

One can see in Fig. 3 that the hindrance to fusion increases at lower energies $E_{c.m.} < 205$ MeV because at these low energies the collisions with small orientation angles (α_P projectile and α_T target) of the axial symmetry axes of colliding nuclei relative to the beam direction [20,36] can only contribute. At the capture of colliding nuclei with small orientation angles α_P and α_T, the intrinsic barrier B^*_{fus} for the transformation into the compound nucleus is large [20]. Therefore, at energies $E_{c.m.} < 205$ MeV the capture of the projectile by the target nucleus in collisions with large orientation angles α_P and α_T is impossible: the initial collision energy is not sufficient to overcome the Coulomb barrier which is large in comparison with the one in the case of small orientation angles. So, the hindrance to complete fusion depends on the orientation angles: the more elongated shape of the DNS formed at collisions with small orientation angles (tip-to-tip configurations) promotes the quasifission rather than the formation of the compound nucleus [20,36]. Therefore, a sufficiently high collision energy $E_{c.m.}$ (as compared with the Bass barrier) was chosen in the experiments aiming for the synthesis of superheavy elements in "hot-fusion" reactions with ^{48}Ca on the actinide nuclei Pu, Am, Cm, Bk, and Cf with the purpose of including the contributions of large orientation angles of the axial symmetry of the target nucleus.

Theoretical results of the ER cross sections for the synthesis of the element $Z = 117$ are compared with experiment in Fig. 4. In this figure, the full squares show experimental data of the ER cross sections measured for the ^{48}Ca+^{249}Bk reaction in Ref. [34]; the curves show theoretical results obtained in this work for the $2n$ (dashed line), $3n$ (solid line), $4n$ (dotted-dashed line), and $5n$ channels (dotted line) by the DNS and advanced statistical models by using the mass tables of Möller and Nix [29] (thick lines) and of Warsaw Group [30] (thin lines).

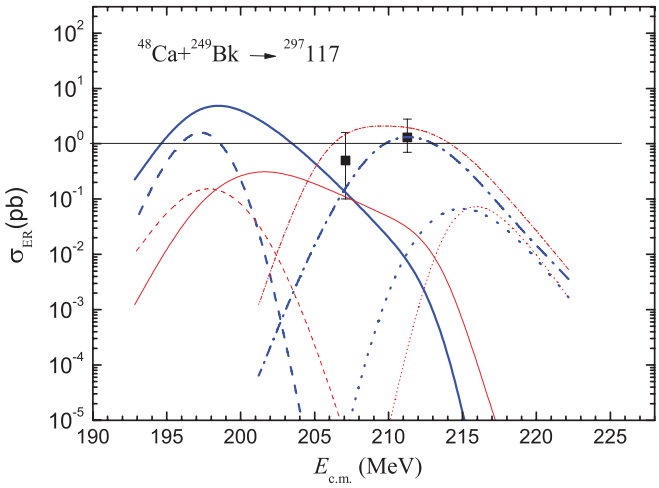

FIG. 4. (Color online) Comparison between the evaporation residue excitation functions for the ^{48}Ca+^{249}Bk reaction calculated by using mass tables of Möller and Nix [29] (thick lines) and of the Warsaw Group [30] (thin lines) for the $2n$ (dashed lines), $3n$ (solid lines), $4n$ (dotted-dashed lines), and $5n$ (dotted lines) channels calculated by the DNS [17,20,33] and advanced statistical [10–12] models. The experimental data of Ref. [34] are presented by squares.

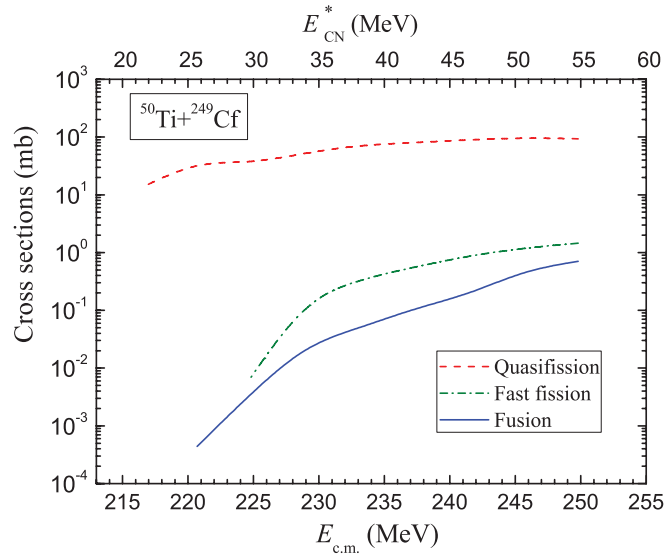

FIG. 5. (Color online) Quasifission (dashed line), fast fission (dotted-dashed line), and complete fusion (solid line) excitation functions calculated by the DNS model [17,20,33] for the ^{50}Ti+^{252}Cf reaction which could lead to the ^{299}120 compound nucleus. The capture cross section is not shown here because it is completely overlapped with the quasifission cross section. The excitation energy E^*_{CN} of the compound nucleus (top axis) is calculated by the use of the Möller and Nix mass table [29].

According to our results, σ_{ER} is larger at the collision energies around $E_{c.m.} = 200$ to 205 MeV. The survival probability W_{surv} of the heated compound nucleus increases with the decrease of its excitation energy.

The main scope of this work is to reproduce the measured data for the superheavy element $Z = 117$ and to make predictions for σ_{ER} in the ^{54}Cr+^{248}Cm and ^{50}Ti+^{249}Cf reactions which can be used in near-future experiments.

In Figs. 5 and 6 we present our theoretical results for quasifission, fast fission, and complete fusion cross sections of the ^{50}Ti+^{249}Cf and ^{54}Cr+^{248}Cm reactions. The capture cross section is not shown in Fig. 5 because it is completely overlapped with the quasifission cross section, since the sum of the fast fission and complete fusion is about two to four orders of magnitude smaller than quasifission cross section. The comparison between these figures shows that, at low energies, the capture cross section in the ^{54}Cr+^{248}Cm reaction is larger than that in the ^{50}Ti+^{249}Cf reaction, while these cross sections become comparable at larger energies. One can also see in these figures that the fusion cross section is sufficiently larger for the ^{50}Ti+^{249}Cf reaction in comparison with the one for the ^{54}Cr+^{248}Cm reaction. The advance of the charge asymmetric system appears at the second stage (fusion) of the reaction mechanism leading to formation of the evaporation residues. It is well known that the hindrance to complete fusion decreases by increasing the DNS charge asymmetry. At the same time the DNS quasifission barrier B_{qf} increases because the Coulomb repulsion forces decrease with the decrease of the product $Z_1 Z_2$. Therefore, in spite of the fact that the ^{50}Ti+^{249}Cf system has less neutrons in comparison with ^{54}Cr+^{248}Cm, the probability of the compound nucleus formation is higher for the former reaction than for the latter one. The more strong hindrance to complete fusion in the case of the ^{54}Cr+^{248}Cm reaction is connected with the larger intrinsic fusion barrier B^*_{fus} and smaller quasifission barrier B_{qf} for this reaction in comparison with ^{50}Ti+^{249}Cf.

The theoretical excitation functions of evaporation residues which can be formed in different neutron-emission channels for these two systems are presented in Figs. 7 and 8. In each of the figures the evaporation residue cross sections for the neutron-emission channels obtained by using binding energies and fission barriers calculated in the microscopic-macroscopic

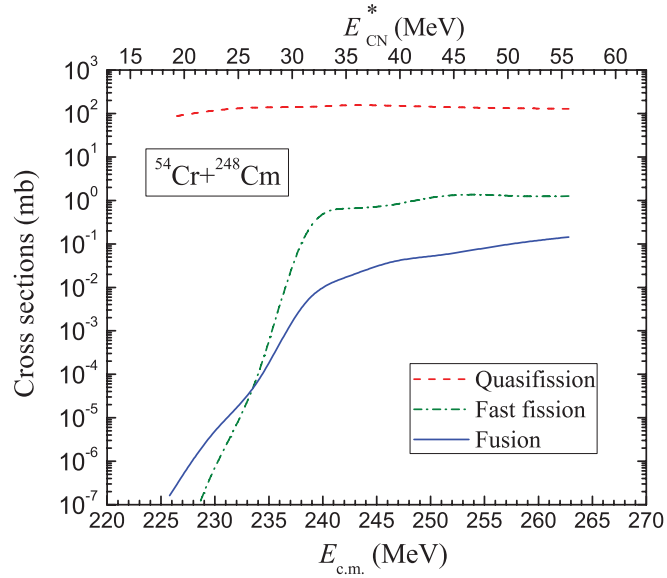

FIG. 6. (Color online) Same as in Fig. 5 but for the ^{54}Cr+^{248}Cm reaction which could lead to the ^{302}120 compound nucleus.

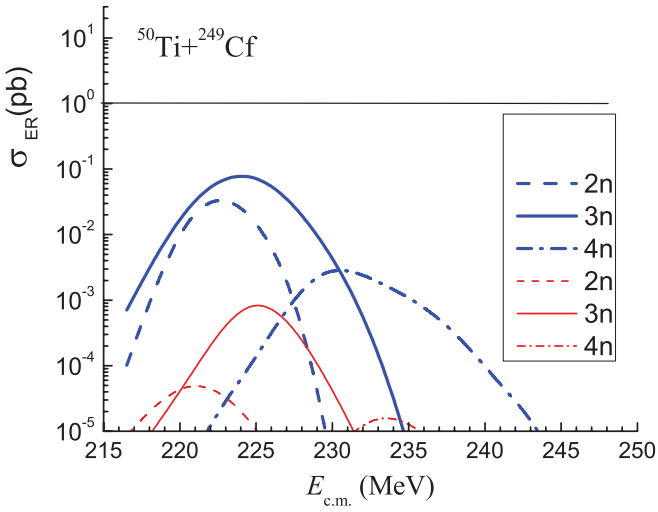

FIG. 7. (Color online) Comparison between the evaporation residue excitation functions for the ^{50}Ti+^{252}Cf reaction calculated by using mass tables of Möller and Nix [29] (thick lines) and of the Warsaw Group [30] (thin lines) for the 2*n* (dashed lines), 3*n* (solid lines), and 4*n* (dotted-dashed lines) channels calculated by the DNS [17,20,33] and advanced statistical [10–12] models.

models of Möller and Nix [29] and of the Warsaw Group [30] are compared. The difference between binding energies obtained by these two groups is in the range 2–3 MeV for the isotopes of superheavy nuclei with $Z > 114$. This difference causes a difference between values of the branching ratios Γ_n/Γ_f which are used in calculations of the survival probability of the heated and rotating nuclei. The use of the binding energies [30] and fission barriers [31,32] of the Warsaw Group leads to two main consequences: the excitation energy of the compound nucleus will be lower because the absolute value of $Q_{gg} = B_{proj} + B_{targ} - B_{CN}$ (negative) is larger: $E^*_{CN} = E_{c.m.} + Q_{gg}$. In this case the fission probability should decrease but the height of the fission barrier calculated

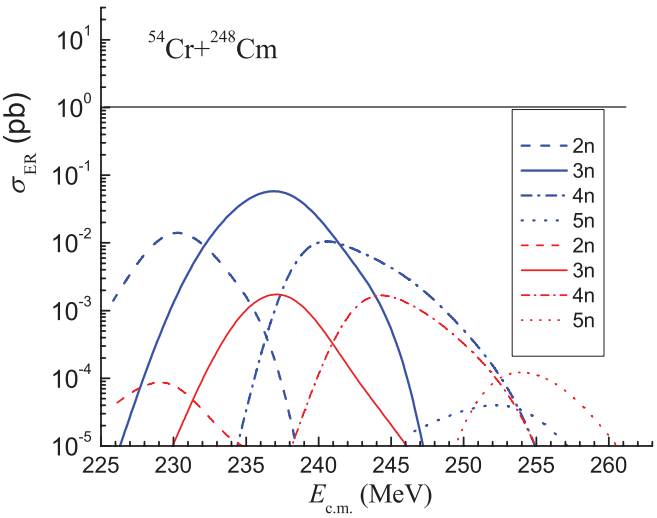

FIG. 8. (Color online) Same as in Fig. 7 but for the ^{54}Cr+^{248}Cm reaction.

by taking into account triaxial deformations significantly decreases by up to 2.5 MeV for the $Z > 112$ [31,32] in comparison with the fission barrier of the Möller and Nix [29] model. The total score is that the fission probability of the CN becomes higher (the survival probability W_{sur} becomes smaller) by the use the binding energies [30] and fission barriers [31,32] of the Warsaw Group in comparison with the case of using the fission barrier of the Möller and Nix [29] model.

Therefore, the evaporation residues cross sections obtained by the use of the mass table calculated by the Nix-Möller microscopic-macroscopic model are one order of magnitude larger in comparison with the results obtained by the use of the mass table of the Warsaw Group.

We should comment on the difference between our present results for the excitation function of evaporation residues σ_{ER} for the *xn* channels in the ^{54}Cr+^{248}Cm reaction and the ones given in Ref. [19]: the values of σ_{ER} presented in Fig. 8 are much lower than those published in Ref. [19]. The analysis showed that the evolution of mass and charge distributions in the DNS constituents was very sensitive to the used nuclear radius parameter r_0. As a result, the drift of the charge distribution to the charge symmetric configuration was underestimated. This circumstance led to overestimation of the fusion factor P_{CN} in the former calculations of σ_{ER} presented in Ref. [19]. We discuss some details in the Appendix.

IV. CONCLUSIONS

In the framework of the combined DNS and advanced statistical models, the ER excitation functions have been calculated for the ^{48}Ca+^{249}Bk reaction and the results are compared with the experimental data given in Ref. [34]. The ER cross section of the 4*n* channel is well described while the 3*n* channel is described in a satisfactory way, in both cases of the used Möller and Nix [29] and Warsaw Group [30] mass tables.

The capture, complete fusion, and evaporation residue excitation functions of the ^{50}Ti+^{252}Cf and ^{54}Cr+^{248}Cm reactions, which could lead to the synthesis of the superheavy element $Z = 120$, have been calculated. The comparison of the results show that at low $E_{c.m.}$ energies the capture cross sections of the ^{54}Cr+^{248}Cm reaction are larger than the ones of the ^{50}Ti+^{249}Cf reaction, while these cross sections become comparable at higher energies corresponding to the 3*n*- and 4*n*-channel formations. The fusion cross section for the ^{50}Ti+^{249}Cf reaction is significantly larger than that for the ^{54}Cr+^{248}Cm reaction, though the former system has a smaller number of neutrons than the latter one. The stronger hindrance to complete fusion in the case of the ^{54}Cr+^{248}Cm reaction is connected with the larger intrinsic fusion barrier B^*_{fus} and smaller quasifission barrier B_{qf} than in the case of the ^{50}Ti+^{249}Cf reaction. In any case, it appears in the present study—when the Möller-Nix mass table is used—that the maximum values of the excitation function corresponding to the 3*n* channel of the evaporation residue formation for the ^{50}Ti+^{249}Cf and ^{54}Cr+^{248}Cm reactions are not higher than 0.1 and 0.07 pb, respectively, while the maximum yield of residue

for the $4n$ channel (0.01 pb) for the reaction induced by ^{54}Cr is higher than the one (0.004 pb) found for the reaction induced by ^{50}Ti.

ACKNOWLEDGMENTS

A.K.N. is grateful to the Istituto Nazionale di Fisica Nucleare and Department of Physics of the University of Messina for the support received in the collaboration between the Dubna and Messina groups, and he thanks the Russian Foundation for Basic Research for the partial financial support in the performance of this work.

APPENDIX

The fusion factor $P_{\rm CN}(E,\ell)$ used in Eq. (3) shows the degree of hindrance to complete fusion due to competition with quasifission. The intense nucleon exchange between constituents of the DNS, which is formed at the capture of the projectile by the target nucleus, can lead to formation of the compound nucleus or quasifission—the DNS breaks down after intense mass transfer from the light constituent to the heavy one. For the heavy systems the hindrance to fusion increases, and $P_{\rm CN}(E,\ell)$ becomes very small in dependence on the mass asymmetry of the entrance channel.

The mass asymmetry degree of freedom may be fully or partially equilibrated [37]. Therefore, while the DNS exists, we have an ensemble $\{Z\}$ of the DNS configurations which contribute to the competition between complete fusion and quasifission with probabilities $\{Y_Z\}$.

The values of $B^*_{\rm fus}$ and $B_{\rm qf}$ are determined from the landscape of the potential energy surface $U(A,Z;R,\ell)$. In Fig. 9 we present their results for the ^{54}Cr+^{248}Cm reaction.

The $P_{\rm CN}$ factor depends on the charge distribution $Y_Z(E^*_{\rm DNS})$:

$$P_{\rm CN}(E^*_{\rm DNS},\ell)=\sum_{Z_{\rm sym}}^{Z_{\rm max}} Y_Z(E^*_{\rm DNS},\ell)P^{(Z)}_{\rm CN}(E^*_{\rm DNS},\ell), \quad \text{(A1)}$$

where $P^{(Z)}_{\rm CN}(E^*_{\rm DNS},\ell)$ is the fusion probability for the DNS having excitation energy $E^*_{\rm DNS}(Z)$ at charge asymmetry Z. The method used to calculate $P^{(Z)}_{\rm CN}(E^*_{\rm DNS},\ell)$ is presented in Ref. [38]. The evolution of Y_Z is calculated by solving the transport master equation:

$$\frac{\partial}{dt}Y_Z(E^*_Z,\ell,t)=\Delta^{(-)}_{Z+1}Y_{Z+1}(E^*_Z,\ell,t)+\Delta^{(+)}_{Z-1}Y_{Z-1}(E^*_Z,\ell,t) - \left(\Delta^{(-)}_Z+\Delta^{(+)}_Z+\Lambda^{\rm qf}_Z\right)Y_Z(E^*_Z,\ell,t), \quad \text{for} \quad Z=2,3,\ldots,Z_{\rm tot}-2. \quad \text{(A2)}$$

Here, the transition coefficients of multinucleon transfer are calculated as in Ref. [39]:

$$\Delta^{(\pm)}_Z=\frac{1}{\Delta t}\sum_{P,T}\left|g^{(Z)}_{PT}\right|^2 n^{(Z)}_{T,P}(t)\left[1-n^{(Z)}_{P,T}(t)\right] \times\frac{\sin^2\left(\Delta t\left(\tilde\varepsilon_{P_Z}-\tilde\varepsilon_{T_Z}\right)/2\hbar\right)}{\left(\tilde\varepsilon_{P_Z}-\tilde\varepsilon_{T_Z}\right)^2/4}, \quad \text{(A3)}$$

where ε_{i_Z} and $n^{(Z)}_i(t)$ are the single-particle energies and occupation numbers of nucleons in the DNS fragments, respectively; and the matrix elements g_{PT} describe one-nucleon exchange between the nuclei of the DNS, and their values are calculated microscopically using the expression obtained in Ref. [40]. In the above-mentioned paper [19], the diffusion of nucleons to the direction of the charge symmetric configuration of the DNS was small due to the smallness of the g_{PT} values which are determined by the mean fields of the interacting nuclei. The radius coefficient $r_0^{\rm mfield}$ used in calculation of the nuclear mean field was smaller in comparison with values of

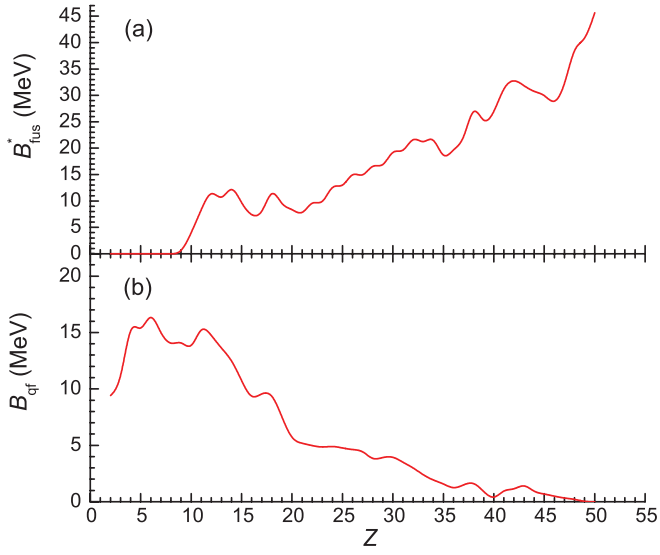

FIG. 9. (Color online) (a) Intrinsic fusion barrier and (b) quasifission barrier as functions of the charge asymmetry for the ^{54}Cr+^{248}Cm reaction.

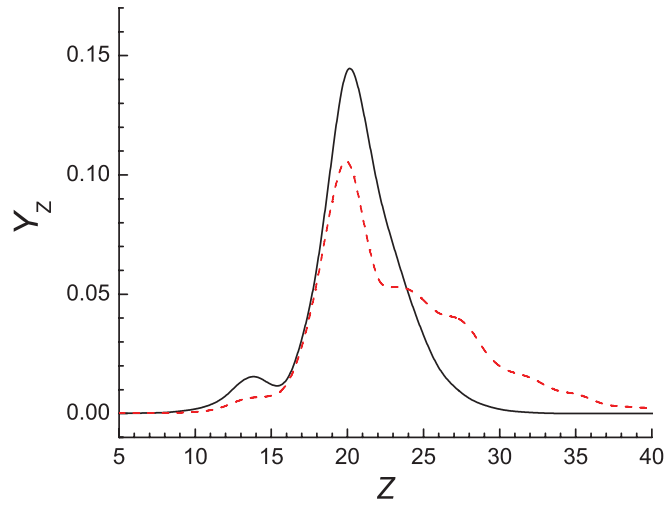

FIG. 10. (Color online) Comparison between the charge distributions in the DNS for the ^{54}Cr+^{248}Cm reaction used in Ref. [19] (dashed line) and in this work (solid line) to calculate the complete fusion cross section.

the radius coefficient r_0^{density} used in calculation of the nucleon density in nuclei. Therefore, when the DNS is formed, the distance between centers is determined by the minimum of the potential well of the nucleus-nucleus interaction, but at this distance the g_{PT} values were small. This fact was not adequately considered in our previous calculation presented in the paper [19]. In Fig. 10, we present the results of the charge distributions in the DNS for the ^{54}Cr + ^{248}Cm reaction.

[1] Yu. Ts. Oganessian *et al.*, Phys. Rev. C **70**, 064609 (2004).
[2] Yu. Ts. Oganessian *et al.*, Phys. Rev. C **74**, 044602 (2006).
[3] S. Hofmann, F. P. Heßberger, V. Ninov, P. Armbruster, G. Münzenberg, C. Stodel, A. G. Popeko, A. V. Yeremin, S. Saro, and M. Leino, Z. Phys. A **358**, 377 (1997).
[4] Kosuke Morita *et al.*, J. Phys. Soc. Jpn. **76**, 043201 (2007).
[5] G. Giardina, S. Hofmann, A. I. Muminov, and A. K. Nasirov, Eur. Phys. J. A **8**, 205 (2000).
[6] Avazbek Nasirov, Giorgio Giardina, Giuseppe Mandaglio, Marina Manganaro, and Werner Scheid, J. Phys.: Conf. Ser. **282**, 012010 (2011).
[7] G. Fazio, G. Giardina, A. Lamberto, R. Ruggeri, C. Saccà, R. Palamara, A. I. Muminov, A. K. Nasirov, U. T. Yakhshiev, and F. Hanappe, Eur. Phys. J. A **19**, 89 (2004).
[8] N. V. Antonenko, E. A. Cherepanov, A. K. Nasirov, V. P. Permjakov, and V. V. Volkov, Phys. Lett. B **319**, 425 (1993); Phys. Rev. C **51**, 2635 (1995).
[9] G. G. Adamian, N. V. Antonenko, and W. Scheid, Phys. Rev. C **68**, 034601 (2003).
[10] A. D'Arrigo, G. Giardina, M. Herman, and A. Taccone, Phys. Rev. C **46**, 1437 (1992).
[11] A. D'Arrigo, G. Giardina, M. Herman, A. V. Ignatyuk, and A. Taccone, J. Phys. G **20**, 365 (1994).
[12] R. N. Sagaidak *et al.*, J. Phys. G **24**, 611 (1998).
[13] G. Fazio *et al.*, J. Phys. Soc. Jpn. **72**, 2509 (2003).
[14] G. Fazio *et al.*, J. Phys. Soc. Jpn. **74**, 307 (2005).
[15] B. B. Back R. R. Betts, J. E. Gindler, B. D. Wilkins, S. Saini, M. B. Tsang, C. K. Gelbke, W. G. Lynch, M. A. McMahan, and P. A. Baisden, , Phys. Rev. C **32**, 195 (1985).
[16] J. Dvorak *et al.*, Phys. Rev. Lett. **100**, 132503 (2008).
[17] G. Fazio *et al.*, Phys. Rev. C **72**, 064614 (2005).
[18] A. Sobiczewski and K. Pomorski, Prog. Part. Nucl. Phys. **58**, 292 (2007).
[19] A. K. Nasirov, G. Giardina, G. Mandaglio, M. Manganaro, F. Hanappe, S. Heinz, S. Hofmann, A. I. Muminov, and W. Scheid, Phys. Rev. C **79**, 024606 (2009).
[20] Avazbek Nasirov, Akira Fukushima, Yuka Toyoshima, Yoshihiro Aritomo, Akhtam Muminov, Shuhrat Kalandarov, and Ravshanbek Utamuratov, Nucl. Phys. A **759**, 342 (2005).
[21] S. Hofmann, F. P. Heßberger, V. Ninov, P. Armbruster, G. Münzenberg, C. Stodel, A. G. Popeko, A. V. Yeremin, S. Saro, and M. Leino, Z. Phys. A **358**, 377 (1997).
[22] L. Stavsetra, K. E. Gregorich, J. Dvorak, P. A. Ellison, I. Dragojević, M. A. Garcia, and H. Nitsche, Phys. Rev. Lett. **103**, 132502 (2009).
[23] S. Hofmann *et al.*, GSI Scientific Report No. PHN-NUSTAR-SHE-01, 2010.
[24] Z. H. Liu and Jing-Dong Bao, Phys. Rev. C **80**, 054608 (2009).
[25] Valery Zagrebaev and Walter Greiner, Phys. Rev. C **78**, 034610 (2008).
[26] G. G. Adamian, N. V. Antonenko, and W. Scheid, Eur. Phys. J. A **41**, 235 (2009).
[27] Yu. Ts. Oganessian *et al.*, Phys. Rev. C **79**, 024603 (2009).
[28] K. Siwek-Wilczyńska, T. Cap, and J. Wilczyński, Int. J. Mod. Phys. E **19**, 500 (2010).
[29] P. Möller and J. R. Nix, J. Phys. G: Nucl. Part. Phys. **20**, 1681 (1994).
[30] I. Muntian, Z. Patyk, and A. Sobiczewski, Phys. At. Nucl. **66**, 1015 (2003).
[31] M. Kowal and A. Sobiczewski, Int. J. Mod. Phys. E **18**, 914 (2009).
[32] M. Kowal, P. Jachimowicz, and A. Sobiczewski, Phys. Rev. C **82**, 014303 (2010).
[33] G. Fazio, G. Giardina, G. Mandaglio, F. Hanappe, A. I. Muminov, A. K. Nasirov, W. Scheid, and L. Stuttgé, Mod. Phys. Lett. A **20**, 391 (2005).
[34] Yu. Ts. Oganessian *et al.*, Phys. Rev. Lett. **104**, 142502 (2010).
[35] G. G. Adamian, R. V. Jolos, A. K. Nasirov, and A. I. Muminov, Phys. Rev. C **56**, 373 (1997).
[36] D. J. Hinde, M. Dasgupta, J. R. Leigh, J. P. Lestone, J. C. Mein, C. R. Morton, J. O. Newton, and H. Timmers, Phys. Rev. Lett. **74**, 1295 (1995).
[37] R. Bock *et al.*, Nucl. Phys. A **388**, 334 (1982).
[38] A. K. Nasirov, A. I. Muminov, R. K. Utamuratov, G. Fazio, G. Giardina, F. Hanappe, G. Mandaglio, M. Manganaro, and W. Scheid, Eur. Phys. J. A **34**, 325 (2007).
[39] R. V. Jolos, A. I. Muminov, and A. K. Nasirov, Yad. Fiz. **44**, 357 (1986); Sov. J. Nucl. Phys. **44**, 228 (1986).
[40] G. G. Adamian, R. V. Jolos, and A. K. Nasirov, Yad. Fiz. **55**, 660 (1992); Sov. J. Nucl. Phys. **55**, 366 (1992).